Inorg. Chem. **2003**, *42*, 3237–3244

New Structural Motifs in the Aggregation of Neutral Gold(I) Complexes: Structures and Luminescence from (Alkyl isocyanide)AuCN

Rochelle L. White-Morris, Matthias Stender, Dino S. Tinti, and Alan L. Balch*

Department of Chemistry, University of California, Davis, California 95616

Daniel Rios and Saeed Attar*

Department of Chemistry, California State University, Fresno, California 93740

Received December 2, 2002

The preparation and X-ray crystal structures of (CyNC)Au^{I}CN, (*n*-BuNC)Au^{I}CN, and (*i*-PrNC)Au^{I}CN·0.5CH_2Cl_2 are reported and compared with those of (MeNC)Au^{I}CN and (*t*-BuNC)Au^{I}CN, which were previously described. These linear molecules are all organized through aurophilic interactions into three structural classes: simple chains ((CyNC)-Au^{I}CN and (*t*-BuNC)Au^{I}CN), side-by-side chains in which two strands make Au···Au contact with each other ((*n*-BuNC)Au^{I}CN), and nets in which multiple aurophilic interactions produce layers of gold(I) centers ((*i*-PrNC)Au^{I}CN and (MeNC)Au^{I}CN). All of these five solids dissolve to produce colorless, nonluminescent solutions with similar UV/vis spectra. However, each of the solids displays a unique luminescence with emission maxima occurring in the range 371–430 nm.

Introduction

Attractive interactions between closed-shell gold(I) centers are important in determining the structures of many gold(I) complexes.[1,2] Such aurophilic interactions are found whenever adjacent Au···Au contacts are less than the van der Waals separation of ca. 3.6 Å.[3−5] Theoretical studies have shown that this weakly bonding interaction is the result of a combination of correlation and relativistic effects,[6−9] while experimental studies of rotational barriers have demonstrated that the strength of this attractive interaction is comparable to hydrogen bonding: ca. 7−11 kcal/mol.[10,11] As a consequence of such aurophilic attractions, many two-coordinate gold(I) complexes self-associate into dimers, trimers, and extended chains that are connected exclusively through Au···Au contacts.

Two-coordinate gold(I) complexes typically are colorless but may display strong luminescence in the visible region of the spectrum depending upon the ligands present and the state of aggregation.[12−14] Patterson and co-workers have shown that the simple $[Au(CN)_2]^-$ and $[Ag(CN)_2]^-$ ions aggregate under a variety of conditions and that the aggregated forms show remarkable variations in their luminescence.[15−17] For example, the luminescence from solutions of $K[Au(CN)_2]$ can be "tuned" to occur from 275 to 470 nm depending upon the concentration and solvent.[18]

* Authors to whom correspondence should be addressed. E-mail: albalch@ucdavis.edu (A.L.B.); sattar@csufresno.edu (S.A.).

(1) Jones, P. G. *Gold Bull.* **1986**, *19*, 46; **1983**, *16*, 114; **1981**, *14*, 159; **1981**, *14*, 102.
(2) Pathaneni, S. S.; Desiraju, G. R. *J. Chem. Soc., Dalton Trans.* **1993**, 319.
(3) Schmidbaur, H. *Gold: Progress in Chemistry, Biochemistry and Technology*; Wiley: New York, 1999.
(4) Grohmann, A.; Schmidbaur, H. In *Comprehensive Organometallic Chemistry II*; Abel, E. W., Stone, F. G. A., Wilkinson, G., Eds.; Elsevier: Oxford, 1995; Vol. 3, p 1.
(5) Puddephatt, R. J. In *Comprehensive Coordination Chemistry*; Wilkinson, G., Gillard, R. D., McCleverty, J. A., Eds.; Pergamon Press: Oxford, 1987; Vol. 5, p 861.
(6) Pyykkö, P.; Runeberg, N.; Mendizabal, F. *Chem. Eur. J.* **1997**, *3*, 1451.
(7) Pyykkö, P.; Mendizabal, F. *Chem. Eur. J.* **1997**, *3*, 1458.
(8) Pyykkö, P. *Chem. Rev.* **1997**, *97*, 597.
(9) Pyykkö, P.; Li, J.; Runeberg, N. *Chem. Phys. Lett.* **1994**, *218*, 133.
(10) Schmidbaur, H.; Graf, W.; Müller, G. *Angew. Chem., Int. Ed. Engl.* **1988**, *27*, 417.
(11) Harwell, D. E.; Mortimer, M. D.; Knobler, C. B.; Anet, F. A. L.; Hawthorne, M. F. *J. Am. Chem. Soc.* **1996**, *118*, 2679.
(12) Forward, J. M.; Fackler, J. P. Jr.; Assefa, Z. In *Optoelectronic Properties of Inorganic Compounds*; Roundhill, D. M., Fackler, J. P., Jr, Eds.; Plenum Press: New York, 1999; p 195.
(13) Yam, V. W. W.; Lo, K. K. W. *Chem. Soc. Rev.* **1999**, *28*, 323.
(14) Leung, K. H.; Phillips, D. L.; Tse, M. C.; Che, C. M.; Miskowski, V. M. *J. Am. Chem. Soc.* **1999**, *121*, 4799.
(15) Rawashdeh-Omary, M. A.; Omary, M. A.; Patterson, H. H. *J. Am. Chem. Soc.* **2000**, *122*, 10371.
(16) Rawashdeh-Omary, M. A.; Omary, M. A.; Shankle, G. E.; Patterson, H. H. *J. Phys. Chem. B* **2000**, *104*, 6143.
(17) Omary, M. A.; Patterson, H. H. *J. Am. Chem. Soc.* **1998**, *120*, 7696.

10.1021/ic0206948 CCC: $25.00
Published on Web 04/04/2003

Table 1. Selected Interatomic Distances and Angles

	(CyNC)AuCN	(*t*-BuNC)AuCN[a]	(*n*-BuNC)AuCN	(*i*-PrNC)AuCN·0.5CH_2Cl_2	(MeNC)AuCN[b]
Au···Au	3.426(3)	3.568	3.3233(3)	3.3209(3)	3.524(4)
	3.442(3)		3.3729(4)	3.3500(4)	3.593(3)
			3.3735(3)	3.4875(3)	3.724(3)
			3.4703(3)	3.4715(3)	
				3.6856(4)	
				3.3500(4)	
				3.4387(4)	
				3.6662(5)	
Au(1)−C(CN)	2.01(2)	2.00(2)	1.985(4)	1.997(6)	2.01(4)
Au(2)−C(CN)				1.994(6)	
Au(3)−C(CN)				1.987(6)	
Au(1)−C(iso)	1.985(17)	1.93(3)	1.985(4)	1.977(6)	1.98(5)
Au(2)−C(iso)				1.988(6)	
Au(3)−C(iso)				1.990(6)	
C−N(CN)	1.10(3)	1.09(3)	1.164(5)	1.139(8)	1.15(6)
C−N(CN)				1.144(7)	
C−N(CN)				1.146(8)	
C−N(iso)		1.21(3)	1.133(5)	1.136(7)	1.18(6)
C−N(iso)	1.13(2)			1.132(7)	
C−N(iso)				1.132(8)	
Au···Au···Au	127.89(7)	130.1	62.425(8)	67.074(8)	59.4
			59.57(1)	56.84(1)	120.6
				26.59(1)	63.1
				42.80(1)	57.5
				150.48(1)	
				17.16(1)	
C−Au(1)−C	178.3(8)	178.2(8)	175.20(13)	174.8(2)	176(2)
C−Au(2)−C				173.8(2)	
C−Au(3)−C				178.9(3)	
Au(1)−C−N(CN)	178(2)	172(2)	177.7(3)	175.7(5)	175(4)
Au(2)−C−N(CN)				179.1(5)	
Au(3)−C−N(CN)				179.7(6)	
Au(1)−C−N(iso)	174.3(17)	175(2)	177.5(3)	174.5(5)	179(4)
Au(2)−C−N(iso)				175.9(5)	
Au(3)−C−N(iso)				177.7(5)	

[a] Data from ref. wr. [b] Data from ref. 23.

Related studies have shown that solutions of the colorless gold carbene complex $[Au\{C(NHMe)_2\}_2](PF_6)\cdot 0.5$(acetone), which are nonluminescent at room temperature, become luminescent upon freezing.[19] The luminescence from these frozen solutions ranges from blue to orange to nonluminescent depending upon the solvent. The solid-state structures of $[Au\{C(NHMe)_2\}_2](PF_6)\cdot 0.5$(acetone) and related salts reveal that this cation can associate through Au···Au interactions to form extended chains or discrete dimers and that the mode of aggregation in the solids depends upon the anion present.[19,20]

Additionally, the cation in $[(CyNC)_2Au^I](PF_6)$ self-associates to form two crystalline polymorphs: a colorless polymorph with linear chains of cations and a short Au···Au contact (3.1822(3) Å), and a yellow polymorph with four independent cations forming kinked, infinite chains and very short Au···Au contacts of 2.9800(5), 2.9784(5), 2.9652(5), and 2.9648(5) Å.[21,22] The polymorphs are both luminescent, λ_{max}: colorless, 424 nm; yellow, 480 nm at 298 K. Colorless solutions of the two polymorphs have identical absorption spectra and are nonluminescent at room temperature. However, freezing solutions of $[(CyNC)_2Au^I](PF_6)$ produces intense luminescence which varies depending upon the solvent involved. Aggregation of the cations is implicated because the luminescence of the frozen state occurs only in relatively concentrated solutions of the complexes.

In order to provide models for the types of aggregation that two-coordinate gold(I) complex can undergo, we have undertaken structural and spectroscopic studies of a series of neutral complexes of the type $(RNC)Au^ICN$. We focused on neutral complexes in the belief that these molecules were more likely to self-associate than either cations or anions, and hence a greater array of modes of association might be observed with such compounds. Two such complexes, $(MeNC)Au^ICN$[23] and $(t\text{-BuNC})Au^ICN$,[24] have been structurally characterized in earlier work, and their structures are discussed in the context of the new structures reported here. The UV/vis absorption spectra and the luminescence of all of these complexes are reported here.

Results

The new, colorless complexes, $(CyNC)Au^ICN$, $(n\text{-BuNC})Au^ICN$, and $(i\text{-PrNC})Au^ICN$, were prepared by the addition

(18) Rawashdeh-Omary, M. A.; Omary, M. A.; Patterson, H. H.; Fackler, J. P., Jr. *J. Am. Chem. Soc.* **2001**, *123*, 11237.
(19) White-Morris, R. L.; Olmstead, M. M.; Jiang, F.; Tinti, D. S.; Balch, A. L. *J. Am. Chem. Soc.* **2002**, *124*, 2327.
(20) White-Morris, R. L.; Olmstead, M. M.; Jiang, F.; Balch, A. L. *Inorg. Chem.* **2002**, *41*, 2313.
(21) White-Morris, R. L.; Olmstead, M. M.; Balch, A. L. *J. Am. Chem. Soc.* **2003**, *125*, 1033.
(22) However, Schmidbaur and co-workers found that other colorless bis(isonitrile)gold(I) complexes, $[(RNC)_2Au^I]X$ (R = methyl, phenyl, and mesityl, and X = triflate or tetrafluoroborate), self-associated only with R = methyl, and in that one case the Au···Au interaction is quite long, 3.624 Å. See: Schneider, W.; Sladek, A.; Bauer, A.; Angermaier, K.; Schmidbaur, H. *Z. Naturforsch. B* **1997**, *52*, 53.
(23) Esperås, S. *Acta Chem. Scand.* **1976**, *A 30*, 527.
(24) Che, C.-M.; Yip, H.-K.; Wong, W.-T.; Lai, T.-F. *Inorg. Chim. Acta* **1992**, *197*, 177.

Table 2. Crystallographic Data

	(CyNC)AuCN	(*n*-BuNC)AuCN	(*i*-PrNC)AuCN·0.5CH_2Cl_2
empirical formula	$C_8H_{11}AuN_2$	$C_6H_9AuN_2$	$C_{5.5}H_8AuClN_2$
fw	332.15	306.12	334.55
color, habit	colorless, needle	colorless, needle	colorless, block
cryst syst	monoclinic	monoclinic	monoclinic
space group	$P2_1/c$	$C2/c$	$P2/c$
a, Å	6.169(7)	21.828(2)	10.9649(6)
b, Å	6.681(7)	10.9685(9)	12.3442(7)
c, Å	22.27(2)	6.7094(5)	16.9844(10)
β, deg	93.65(3)	103.975(3)	95.4050(10)
V, Å^3	916.0(16)	1558.8(2)	2288.7(2)
Z	4	8	12
T/K	200(2)	90(2)	90(2)
λ, Å	0.71073	0.71073	0.71073
ρ/g cm^{-1}	2.409	2.609	2.663
μ/mm^{-1}	16.000	18.790	19.310
R1[a] (obsd data)	0.0660	0.0187	0.0313
wR2[a] (all data, F^2 refinement)	0.185	0.0395	0.0808

[a] $R1 = \Sigma||F_o| - |F_c||/\Sigma|F_o|$; $wR2 = [\Sigma[w(F_o^2 - F_c^2)^2]/\Sigma[w(F_o^2)^2]]^{1/2}$.

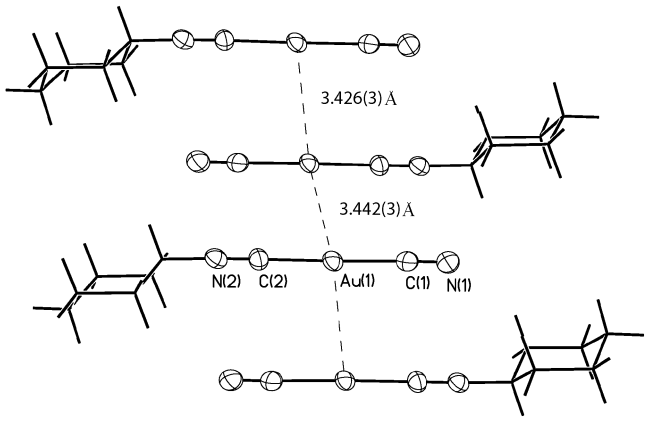

Figure 1. A view of a chain of molecules in (CyNC)Au^{I}CN.

of the appropriate isocyanide to a suspension of AuCN in chloroform. After all of the solid had dissolved, the product was precipitated by the addition of petroleum ether. Examination of the crystalline solids by X-ray diffraction revealed that the C−N−C−Au−C−N portions of the individual molecules are all nearly linear, and there are no notable variations in the internal distances and angles within the molecules. Table 1 contains selected interatomic distances and angles. The crystal data are set out in Table 2.

However, the organization of the individual molecules in each solid differs. Broadly, the molecules organized themselves into three structural classes: simple chains, side-by-side chains in which two strands made additional contacts with each other, and nets in which multiple aurophilic interactions produced layers of gold(I) centers.

Simple Chains: (CyNC)Au^{I}CN and (*t*-BuNC)Au^{I}CN. The structure of (CyNC)Au^{I}CN reveals that there is one molecule in the asymmetric unit which associates to form a one-dimensional infinite chain. Figure 1 shows a drawing of the structure. Individual molecules pack about centers of symmetry to form a zigzag chain with an Au···Au···Au angle of 127.89(7)° and two alternating Au···Au distances of 3.426(3) and 3.442(3) Å. This zigzag chain formation is similar to that found in (*t*-BuNC)Au^{I}CN which has an Au···Au···Au angle of 130.1° and one slightly longer Au···Au distance of 3.568 Å.[24]

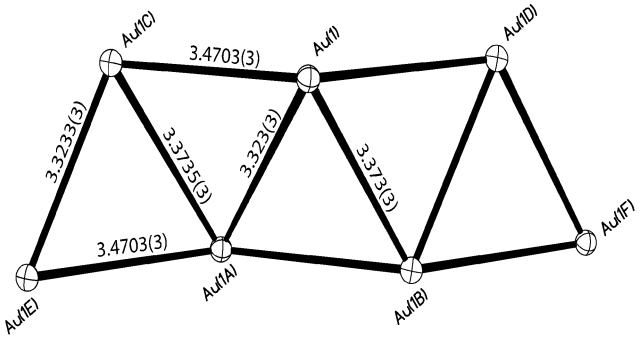

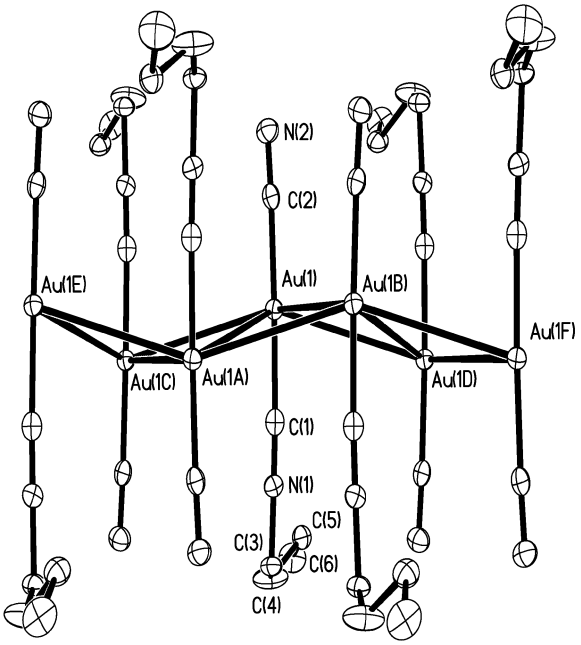

Figure 2. A drawing showing the interactions between molecules in crystalline (*n*-BuNC)Au^{I}CN. Hydrogen atom positions are omitted.

Side-by-Side Chains: (*n*-BuNC)Au^{I}CN. The structure of (*n*-BuNC)Au^{I}CN also consists of one molecule in the asymmetric unit, but crystallographic symmetry produces a more complex pattern of aggregation. Figure 2 shows how these molecules are arranged. The structure can be viewed as an arrangement of two parallel, but slightly bent, chains

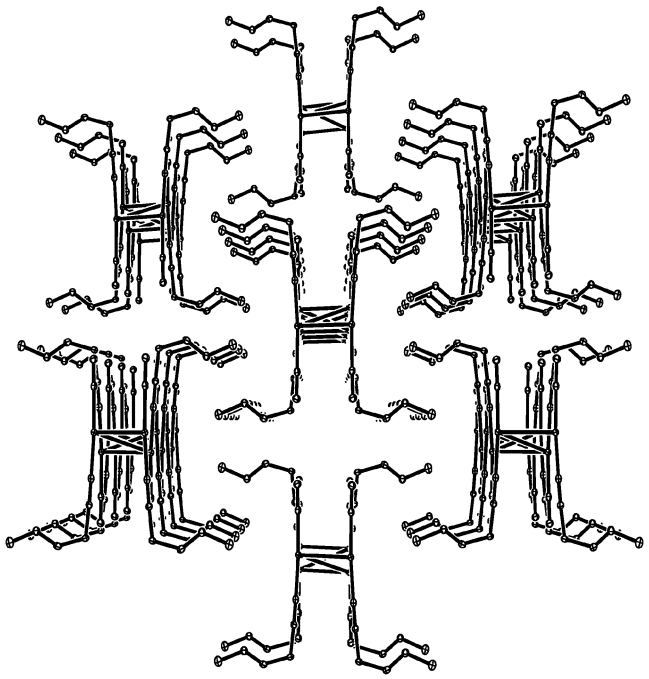

Figure 3. A view of the structure of crystalline (*n*-BuNC)Au^{I}CN which shows how the pairs of chains are insulated from one another. Hydrogen atom positions are omitted.

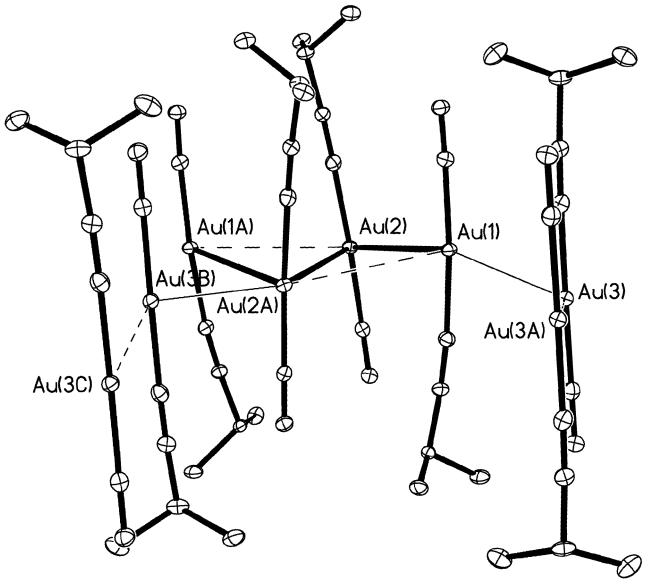

Figure 4. A view of the supramolecular structure of (*i*-PrNC)Au^{I}CN·0.5CH_2Cl_2. Hydrogen atom positions are omitted.

of gold complexes. Within each chain the gold centers are connected through Au···Au contacts of 3.4703(3) Å. In Figure 2, one chain consists of Au(1C), Au(1), and Au(1D), while the other consists of Au(1E), Au(1A), Au(1B), and Au(1F). Au(1) is transformed into Au(1C) or into Au(1D) through crystallographic centers of symmetry. Within these chains the angle Au···Au···Au is 150.3(1)°. These two chains are connected to one another through additional aurophilic interactions. These Au···Au contacts are shorter than the contacts within the chains. Thus, Au(1) is transformed into Au(1A) by a crystallographic center of inversion to produce a Au···Au contact of 3.3233(3) Å, while Au(1) is transformed into Au(1B) by a crystallographic 2-fold axis to produce a Au···Au contact of 3.3735(3) Å. As a result of these aurophilic interactions, each gold ion in (*n*-BuNC)-Au^{I}CN is connected to four other gold(I) ions through Au···Au contacts that are shorter than 3.6 Å.

Figure 3 shows a view of the structure of (*n*-BuNC)-Au^{I}CN that reveals that the side-by-side chains are isolated from each other. The *n*-Bu groups protrude away from the chains and effectively insulate one chain from its neighbors. There is disorder in the positions of the γ and δ carbon atoms of the butyl group. The two alternative positions for each of these carbon atoms have 0.50 site occupancy. Only one of these sites is shown in Figures 2 and 3.

Nets: (*i*-PrNC)Au^{I}CN·0.5CH_2Cl_2 and (MeNC)Au^{I}CN. Unlike the compounds considered previously, the solid-state structure of (*i*-PrNC)Au^{I}CN·0.5CH_2Cl_2 involves three crystallographically different molecules in the asymmetric unit. As noted above, however, the three molecules show only minor variations in their geometric parameters. Figures 4 and 5 show how these three different molecules interact with one another. The molecules are arranged in layers with aurophilic interactions running through the centers of each layer. Figure 5 shows the network of aurophilic interactions that are present within a layer. The shortest Au···Au contacts (3.3209(3) and 3.3500(4) Å) are found between molecules containing Au(1) and Au(2). Two molecules containing Au-(2) and two molecules containing Au(1) are arranged about a crystallographic 2-fold axis to form an aggregate with a Z shape as seen in the bold outline in Figure 5. These figure Z arrangements are connected through further contacts involving, for example, Au(1A) and Au(1B) to create extended and strongly bent chains. Molecules containing Au-(3) are appended to edges of these chains through Au···Au interactions with both Au(1) (at 3.4715(3) Å) and Au(2) (at 3.4875(3) Å). Finally, molecules containing Au(3) are also packed about crystallographic centers of symmetry to connect the units described above. The Au···Au separations here are larger, 3.6662(5) Å, just at the edge where such interactions are viewed as significantly attractive.

As reported earlier, crystalline (MeNC)Au^{I}CN also forms a sheetlike structure.[23] However, in this solid there is only one molecule in the asymmetric unit. Each gold atom is surrounded by six other gold ions in a roughly hexagonal arrangement which involves Au···Au contacts at 3.524(4), 3.593(3), and 3.724(3) Å.

Spectroscopic Properties. The UV/vis spectra of (CyNC)-Au^{I}CN, (*n*-BuNC)Au^{I}CN, and (*i*-PrNC)Au^{I}CN·0.5CH_2Cl_2 in acetonitrile solution are shown in Figure 6. As expected, the presence of differing alkyl groups produces negligible variation in these spectra, and all resemble the spectrum of (MeNC)Au^{I}CN in solution which was reported by Chastain and Mason.[25] These authors have assigned the intense bands in the ultraviolet to metal-to-ligand charge transfer (MLCT) from the filled gold d orbitals. As they noted, there is no evidence for separate MLCT to the two different types of

(25) Chastain, S. K.; Mason, W. R. *Inorg. Chem.* **1982**, *21*, 3717.

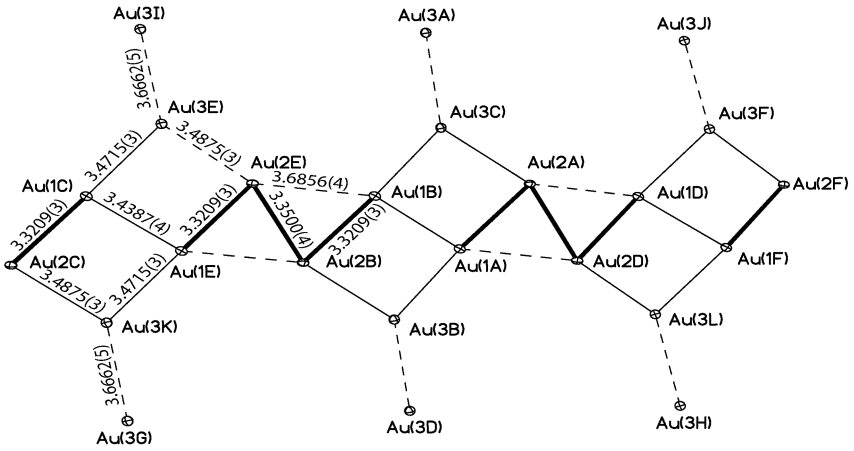

Figure 5. A projection of the layered structure of (*i*-PrNC)Au^{I}CN·0.5CH_2Cl_2 which shows the aurophilic interactions. Hydrogen atom positions are omitted.

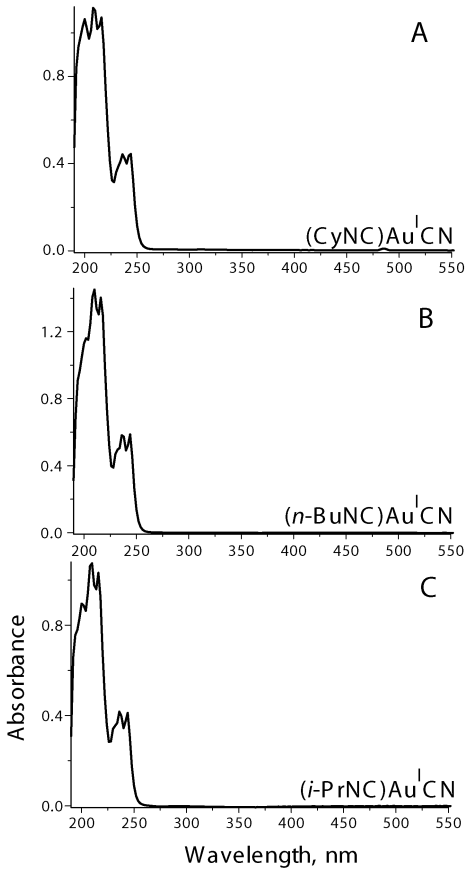

Figure 6. The absorption spectra of 0.18 mM acetonitrile solutions of (A) (CyNC)Au^{I}CN), (B) (*n*-BuNC)Au^{I}CN; and (C) (*i*-PrNC)Au^{I}CN·0.5CH_2Cl_2.

ligands present in these complexes. None of the solutions used to obtain the spectra shown in Figure 6 are luminescent.

However, as solids each of these complexes is luminescent at room temperature. Figure 7 shows the emission and excitation spectra of polycrystalline samples of (CyNC)-Au^{I}CN, (*t*-BuNC)Au^{I}CN, (*n*-BuNC)Au^{I}CN, (*i*-PrNC)Au^{I}CN·0.5CH_2Cl_2, and (MeNC)Au^{I}CN. For (*n*-BuNC)Au^{I}CN, (*i*-PrNC)Au^{I}CN·0.5CH_2Cl_2, and (MeNC)Au^{I}CN the emission is independent of excitation wavelength. However, for (CyNC)Au^{I}CN and (*t*-BuNC)Au^{I}CN there is a wavelength dependence of the emission. Thus, for (CyNC)Au^{I}CN the dashed line in Figure 7 shows the emission spectrum with excitation at 315 nm, which produces an emission maximum at 413 nm. The excitation profile shown was obtained while emission was monitored at 413 nm. Excitation at longer wavelengths produces a shoulder at ca. 460 nm. The solid line in the top panel of Figure 7 shows the emission spectrum obtained with excitation at 360 nm. For (*t*-BuNC)Au^{I}CN two different sets of emission and excitation spectra are shown in Figure 7. The emission spectra are dependent upon the excitation wavelength. The first set of spectra show the emission generated by excitation at 293 nm and the excitation profile for the emission at 371 nm. The second set of spectra show the emission obtained by excitation at 341 nm and the emission profile for the emission at 456 nm. Interestingly, the two solids that show changes in their emission as a function of excitation wavelength belong to the same structural class with simple zigzag chains.

Despite the similarity in the absorption spectra of these complexes, the solid-state luminescence of each shows unique features. The emission maxima range from 371 nm for (*t*-BuNC)Au^{I}CN to 430 nm for (*i*-PrNC)Au^{I}CN, and the excitation maxima range from 293 nm for (*t*-BuNC)Au^{I}CN and (*n*-BuNC)Au^{I}CN to 353 nm for (*i*-PrNC)Au^{I}CN·0.5CH_2Cl_2 and (MeNC)Au^{I}CN. Moreover, the spectra of (CyNC)-Au^{I}CN and (*t*-BuNC)Au^{I}CN show two emission bands. The observation that the excitation maxima occur at lower energies than any of the MLCT absorption features seen in the solution phase spectra shown in Figure 6 indicates that the absorption and emission properties of the solid are supramolecular in nature and that the aurophilic interactions are crucial for the observation of luminescence.

The luminescence decays of the solids were recorded at room temperature following pulsed excitation at 337 nm with a N_2 laser. The decays could be analyzed as a sum of two exponential components, but the shorter-lived component had a small amplitude and significant error in all cases. Its origin is unclear. We present the lifetimes only for the longer-lived component. This component has a lifetime of 140 ns in (MeNC)AuCN. The long-lived components have longer lifetimes in the other solids. For both (*n*-BuNC)AuCN and (CyNC)AuCN the lifetimes are 0.70 μs, and for both (*t*-BuNC)AuCN and (*i*-PrNC)AuCN the lifetimes are 1.2 μs.

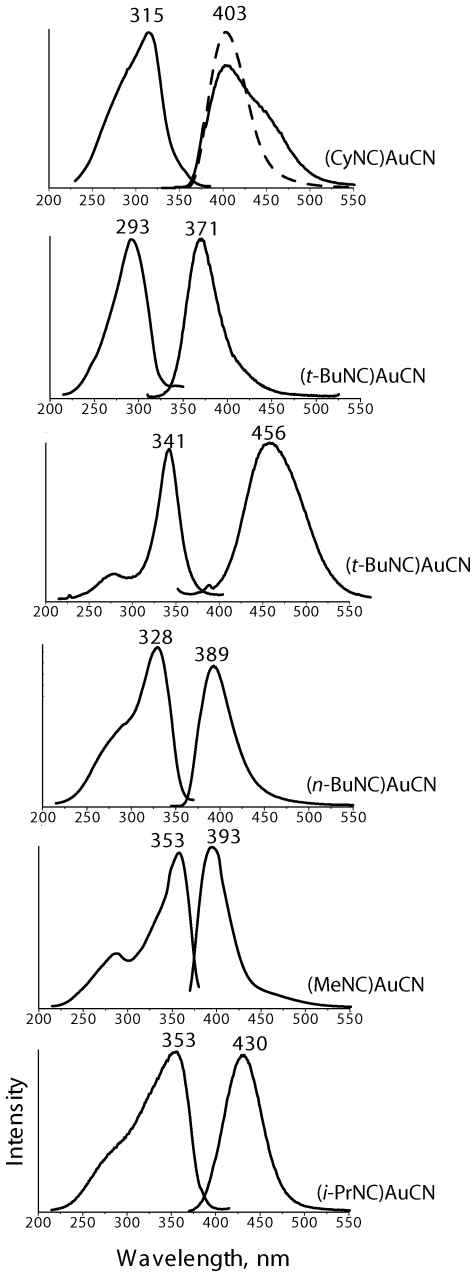

Figure 7. The emission (right) and excitation (left) spectra of crystalline samples of (CyNC)Au^{I}CN, (*t*-BuNC)Au^{I}CN, (*n*-BuNC)Au^{I}CN, (*i*-PrNC)-Au^{I}CN·0.5CH_2Cl_2, and (MeNC)Au^{I}CN obtained at 25 °C. For (CyNC)-Au^{I}CN the dashed line shows emission with excitation at 315 nm and the excitation profile was obtained while emission was monitored at 413 nm. The solid line shows the emission spectrum obtained with excitation at 360 nm. For (*t*-BuNC)Au^{I}CN the first set of spectra show the emission generated by excitation at 293 nm and the excitation profile for the emission at 371 nm, while the second set of spectra show the emission obtained by excitation at 341 nm and the emission profile for the emission at 456 nm.

All reported lifetimes have relative uncertainties of ±10%. These lifetimes suggest that the corresponding components of the emission represent phosphorescence.

The time-resolved emission spectra at 0 ns delay (with 337 nm excitation) agree with the CW emission spectra shown in Figure 7 for (*n*-BuNC)Au^{I}CN, (*i*-PrNC)Au^{I}CN·0.5CH_2Cl_2, and (MeNC)Au^{I}CN and with the CW emission spectra of (CyNC)Au^{I}CN (band at 403 nm, exclusively) and (*t*-BuNC)Au^{I}CN with excitation at 341 nm. The spectra at 150 ns delay (with 337 nm excitation) agree with the data in Figure 7 for (MeNC)AuCN, (*n*-BuNC)AuCN, and (*i*-PrNC)AuCN·0.5CH_2Cl_2. For (CyNC)AuCN and (*t*-BuNC)-AuCN, the spectra at a delay of 150 ns are shifted to longer wavelengths relative to the spectra taken at 0 ns. This shift is more pronounced for (*t*-BuNC)AuCN where the emission maximum shifts from 420 at 0 ns delay to 460 nm at 150 ns delay. In (CyNC)AuCN the emission maximum remains at 405 nm, but a distinct shoulder appears at 460 nm in the spectra at 150 ns delay. These variations are consistent with the differences seen in the effects of excitation wavelength on the emission of (*t*-BuNC)AuCN and (CyNC)AuCN. Interestingly, the two solids that show changes in their time-resolved spectra also belong to the same structural class with simple zigzag chains.

In agreement with the proposition that the spectroscopic properties of the solids are a result of the supramolecular structures present in the crystals, the UV/vis absorption spectra of the solids also differ from those of the solutions. Relevant data are reported in Figure 8, which shows absorption spectra of the complexes recorded as dispersions in KBr.

Infrared spectra of the new complexes, which show clearly differentiated ν(cyanide) and ν(isocyanide) bands, are reported in the Experimental Section.

Discussion

The structural data reported here demonstrate that the neutral molecules, (RNC)Au^{I}CN, can self-associate through aurophilic interactions into a range of different solid-state structures. However, it is interesting to note that none of the close Au···Au separations seen in these *neutral* molecules are as short as those observed between the chains of *cations* in [Au{C(NHMe)$_2$}$_2$](PF$_6$)·0.5(acetone) (Au···Au, 3.1882-(1) Å) and in the two polymorphs of [(CyNC)$_2$Au^{I}](PF$_6$) (colorless, Au···Au, 3.1822(3) Å; yellow, Au···Au, 2.9803-(6), 2.9790(6), 2.9651(6), and 2.9643(6) Å). On the other hand, these neutral rodlike complexes do show interesting variations in their modes of aggregation, which can involve additional aurophilic interactions beyond those seen in chain structures. For example, in (*i*-PrNC)Au^{I}CN·0.5CH_2Cl_2 each of the three crystallographically different gold ions interacts with three neighboring gold ions, whereas in chain aggregates there are, of course, only two neighboring gold ions. In (*n*-BuNC)Au^{I}CN, each gold ion interacts with four other gold ions in the side-by-side chains. In (MeNC)Au^{I}CN, each gold ion interacts with six others in a hexagonal net but the Au···Au distances are longer.

The crystalline forms of all five complexes ((CyNC)-Au^{I}CN, (*t*-BuNC)Au^{I}CN, (*n*-BuNC)Au^{I}CN, (*i*-PrNC)Au^{I}CN·0.5CH_2Cl_2, and (MeNC)Au^{I}CN) are luminescent at room temperature, but their solutions are nonluminescent. Consequently, the luminescence of the solids is attributed to the presence of aurophilic interactions in the solid state. The differences seen in the excitation profiles and the absorption spectra of these complexes reinforce the notion that the luminescence arises from the unique intermolecular interactions present in the solid. The luminescent features (λ_{max}

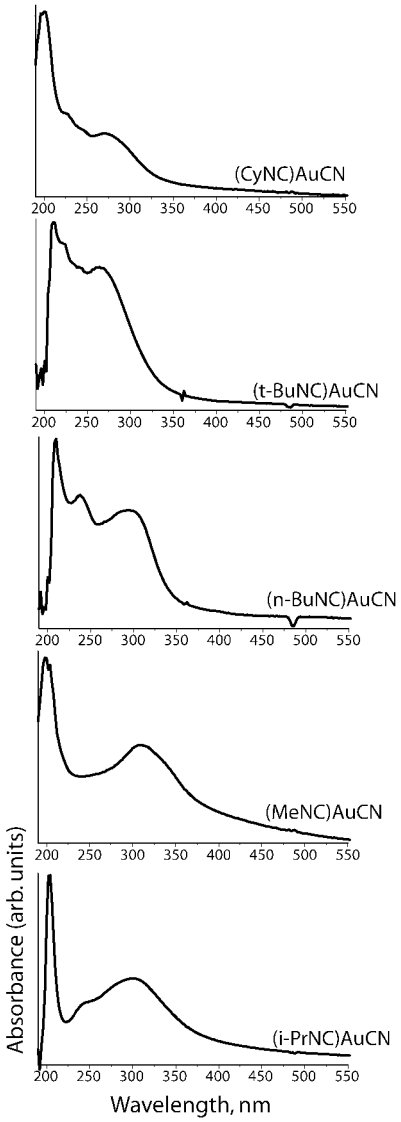

Figure 8. The absorption spectra of crystalline samples of (CyNC)Au^{I}CN, (*t*-BuNC)Au^{I}CN, (*n*-BuNC)Au^{I}CN, (*i*-PrNC)Au^{I}CN·0.5CH_2Cl_2, and (MeNC)Au^{I}CN dispersed in a potassium bromide pellet at 25 °C.

excitation and λ_{max} emission) of each crystalline solid are different, whereas the solution UV/vis spectra of these complexes are nearly identical. Moreover, the two examples ((CyNC)AuCN and (*t*-BuNC)AuCN) from the structural class with simple zigzag chains show similar features in that there are dual emissions that are time-resolved and that show dependence on excitation wavelength.

The aurophilic attractions in these crystals allow overlap of the occupied gold 5d orbitals to produce a filled band of orbitals, while overlap of the empty gold 6p orbitals produces a corresponding band of unoccupied orbitals. Excitation of an electron from the filled 5d band to the empty 6p band strengthens the bonding along these chains by removing what is effectively an antibonding electron from the 5d band and transferring that electron to the bonding 6p band. Emission results from the reverse process, transfer of an excited electron from the 6p band back to the 5d band.

It is interesting to compare the results reported here to those reported for the binuclear complex, **1** (μ-dmb){AuCN}$_2$ (dbm is 1,8-diisocyano-*p*-menthane).[26] In this complex the

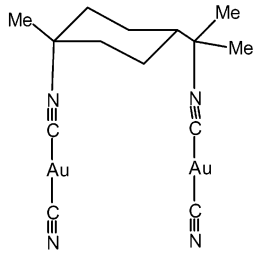

1, (μ-dmb){AuCN}$_2$

bridging dmb ligand facilitates the aurophilic interaction. The intramolecular Au···Au separation in the solid state is 3.54-(1) Å. This binuclear complex is luminescent in solution (λ_{max} = 458 nm in dichloromethane), since the bridging ligand can maintain the aurophilic interaction upon dissolution. Isoelectronic acetylide complexes of the type RNCAuCCR are also luminescent. However, the examples presently known involve arene substituents, and the luminescence from such complexes is likely to arise from ligand $\pi-\pi^*$ states.[27]

Experimental Section

Materials. Gold(I) cyanide, *n*-butyl isocyanide, and *i*-propyl isocyanide were obtained from Strem Chemicals. Cyclohexyl isocyanide was purchased from Aldrich. All chemicals were used as received.

Preparation of (RNC)Au^{I}CN. All compounds were obtained through the same synthetic procedure. Gold cyanide (110 mg, 0.49 mmol) was suspended in 12 mL of chloroform. The respective isocyanide (0.56 mmol) was added to the suspension, and it was stirred for 1 h. During this time, the yellow suspension dissolved to produce a colorless solution. The solution was then filtered, and its volume was reduced to 4 mL under a vacuum. Petroleum ether (ca. 20 mL) was added to the concentrated solution to producing a colorless solid. The solid was collected by filtration, washed with petroleum ether, and dried under a vacuum. The yields of the products were (CyNC)AuCN, 69%; (*i*-PrNC)AuCN, 79%; and (*n*-BuNC)AuCN, 76%.

Crystals of (CyNC)AuCN were obtained from slow evaporation of a dichloromethane solution of the complex, while crystals of (*i*-PrNC)AuCN and (*n*-BuNC)AuCN were grown through liquid diffusion of diethyl ether into a dichloromethane solution of the respective complex.

Infrared Spectra. (CyNC)AuCN: 2943.8, 2918.6, 2856.3, 2256.1 (ν(cyanide)), 2157. 3 (ν(isocyanide)), 1448.4, 1366.2, 894.3 cm^{-1}. (*i*-PrNC)AuCN: 2980.8, 2941.7, 2870.0, 2263.8 (ν(cyanide)), 2156.5 (ν(isocyanide)), 1446.5, 1341.0, 908.2 cm^{-1}. (*n*-BuNC)-AuCN: 2960.5, 2923.0, 2868.9, 2277.7 (ν(cyanide)), 2155.9 (ν-(isocyanide)), 1423.0, 1377.6, 931.2 cm^{-1}. (MeNC)AuCN: 3014.9, 2291.2 (ν(cyanide)), 2155.3 (ν(isocyanide)), 1434.5, 1398.3, 970.2 cm^{-1}.

Physical Measurements. Infrared spectra were recorded as pressed KBr pellets on a Matteson Galaxie Series FTIR 3000 spectrometer. Electronic absorption spectra were recorded using a Hewlett-Packard 8450A diode array spectrophotometer. Conven-

(26) Che, C. M.; Wong, W. T.; Lai, T. F.; Kwong, H. L. *J. Chem. Soc., Chem. Commun.* **1989**, 243.
(27) Irwin, M. J.; Vittal, J. J.; Puddephatt, R. J. *Organometallics* **1997**, *16*, 3541. Jia, G.; Payne, N. C.; Vittal, J. J.; Puddephatt, R. J. *Organometallics* **1993**, *12*, 4771.

tional fluorescence excitation and emission spectra were recorded on a Perkin-Elmer LS50B luminescence spectrophotometer. These spectra were collected at room temperature (298 K) on polycrystalline samples that were examined microscopically to determine that the samples contained crystals of uniform morphology and ones that produced uniform luminescence.

Pulsed excitation for the luminescence decay measurements and the time-resolved spectra was provided by a N_2 laser (337 nm, $\leq$10 ns pulse width). The luminescence intensity following the pulsed excitation was monitored by a 1 m spectrometer with a RCA C31034 photomultiplier. The spectrometer output was processed by a Tektronix TDS 724C digitizing oscilloscope for the decay measurements and a Stanford Research Systems SR250 gated integrator and boxcar averager for the time-resolved spectra. The digitized decay data were analyzed by a least-squares fitting procedure.

X-ray Crystallography and Data Collection. The crystals were removed from the glass tubes in which they were grown together with a small amount of mother liquor and immediately coated with a hydrocarbon oil on the microscope slide. Suitable crystals were mounted on glass fibers with silicone grease and placed in the cold dinitrogen stream of a Bruker SMART CCD with graphite-monochromated Mo Kα radiation at 90(2) K. Crystals of (CyNC)AuCN cracked upon cooling to 90 K, and hence the data for this compound were obtained at 200 K. No decay was observed in 50 duplicate frames at the end of each data collection. Crystal data are given in Table 2.

The structures were solved by direct methods and refined using all data (based on F^2) using the software of SHELXTL 5.1. A semiempirical method utilizing equivalents was employed to correct for absorption.[28] Hydrogen atoms were added geometrically and refined with a riding model.

Acknowledgment. We thank the Petroleum Research Fund (Grant 37056-AC) for support. The Bruker SMART 1000 diffractometer was funded in part by NSF instrumentation grant CHE-9808259.

Supporting Information Available: X-ray crystallographic files in CIF format for (CyNC)Au^{I}CN, (*n*-BuNC)Au^{I}CN, and (*i*-PrNC)Au^{I}CN·0.5CH_2Cl_2. This material is available free of charge via the Internet at http://pubs.acs.org.

IC0206948

(28) SADABS 2.0, Sheldrick, G. M. based on a method of Blessing, R. H. *Acta Crystallogr., Sect. A* **1995**, *A51*, 33.